Near Surface Geophysics, 2012, **10**, xxx-xxx doi:10.3997/1873-0604.2012042

Induced polarization 3D tomography of an archaeological direct reduction slag heap

N. Florsch[1*], M. Llubes[2] and F. Téreygeol[3]

[1]*Université Pierre et Marie Curie, Case 105, 4 place Jussieu, 75252 Paris Cedex 05, France*
[2]*Observatoire Midi-Pyrénées, UMR5563, Toulouse, France*
[3]*CNRS, IRAMAT-LMC, UMR 5060, Belfort, France*

Received April 2011, revision accepted September 2012

ABSTRACT

Both environmentalists and archaeologists are interested in the detection and quantification of the remains of mine slag heaps from ancient smelters: possible pollution of the slag heaps and information concerning the history of the smelter's mine. Although magnetic surveys can be used to detect subsurface slag accumulations, it is not possible to derive the total amount of material from such surveys or to accurately delineate the heaps through the use of this method. Conversely, 'Induced Polarization' (IP) surveying allows a relevant and robust assessment of the volume of slag concentrations to be determined. In the present study, we follow up on results obtained in a previous study, carried out at the 14th Castel-Minier mine (Ariège, France) site, where we have shown that the chargeability is proportional to the slag concentration in the ground and have used this property to perform 3D tomography of the heap. Based on a previous investigation using spectral induced polarization along a simple profile showing that the phase peak related to the slags is situated at approximately 1 Hz, in the present paper we extend our prospection to 3D by using a Terrameter SAS1000 and measuring temporal chargeability. The set of three-dimensional data is recorded by means of classical transect measurements along parallel close profiles and is then interpreted using the RES3DINV code. Finally, archaeological and auger soundings confirmed the assessments derived from this geophysical investigation. We also briefly discuss the source of the IP signal, which we suspect to be induced by magnetite particles embedded in the slags.

INTRODUCTION

Slag heaps are an important form of remains from metallurgical activities and the quantity of slag provides insight into the quantities of metals produced. The technical aspects of the production of metal are a highly important but only recently recognized issue for historians and archaeologists: the power of a nation depends not only on its natural resources but also on its ability to transform raw materials, in particular into coinage (Decombeix *et al.* 1998; Domergue and Leroy 2000).

Although the magnetic method is a very efficient tool for the detection of paleo-metallurgical remains, neither the total (or gradient) field method, nor surface magnetic susceptibility measurements, allow the extent of a heap to be estimated in terms of depth. The estimation of the volume and mass of a slag heap, using non-invasive geophysical methods, is thus still a challenge for scientists.

It should be noted that the application of IP to the archaeological discipline is relatively uncommon. Some pioneering work can be attributed to Aspinal and Lunam (1968a,b), although these authors did not refer to metallurgy. The German team led by Andreas Weller recently developed several applications, one of which is devoted to smelter and slag-heap characterization (Weller 2003; Ullrich *et al.* 2007a). It is important to acknowledge their role in the development of IP for archaeology. If we restrict the scope of these authors' research to that concerning metallurgy, the following authors should be mentioned: Weller *et al.* (2000), Schleifer *et al.* (2002) and more recently, Ullrich *et al.* (2007b). Our own initial experience with archaeological applications, gained in 2005, was reported in Florsch *et al.* (2008) but did not take into account the research work of the German teams, which at that time was unknown to us, although 3D tomography was not new. Indeed, IP applications for the analysis of environmental problems are steadily increasing, especially in situations requiring the study of pollution (Kemna and Binley 1996; Kemna *et al*. 2004).

In the present paper, we investigate the possibilities offered by the Induced Polarization (IP) method, in terms of achieving 3D mass and volume estimations of slag heaps. Although the first study made by our team is reported in Florsch *et al.* (2011), it related to analyses made in 2D, either by surface mapping or verti-

*nicolas.florsch@upmc.fr

cal ERT (Electrical Resistivity Tomography) and did not involve full 3D inversion analysis. In this previous study, thanks to laboratory calibrations used to fit the IP response to the slag concentration, the main outcome was the demonstration of our ability to retrieve the total volume of a slag heap, with an acceptable degree of reliability. The aim of the present paper is to validate and generalize this concept, through a true 3D characterization, applied to ancient metallurgy sites and slag heaps in particular.

The heap investigated in this study lies very close, although several metres away, to the heap investigated in our previous paper, i.e., that described in Florsch *et al.* (2011). The archaeological and geophysical contexts are thus very similar and most of the methods and conclusions used for the study of the first heap can be applied to the second one described here. As an example, we used the same calibration constant found in the previous study to convert the chargeability into a mass concentration, because the slags themselves and their backgrounds are identical.

The principle of IP is to extend the classical Direct Current (DC) electrical method in the time (or equivalently, frequency) domain (Kemna 2000). With respect to IP, DC is simply the IP response when the stationary state has been reached, or equivalently, the electrical response of the ground at zero frequency. However, IP addresses physical phenomena that are considerably richer than those investigated by DC, in terms of the information they can provide, because it involves several polarization mechanisms occurring in a medium and produces a signal that is found to be apparently almost independent of the medium's resistivity. In phenomenological terms, Maxwell's equations apply, involving complex conductivity and permittivity, which are in fact not constant but depend strongly on the frequency range used. 'Traditional' IP is the geophysical vision of what is more generally termed 'impedance spectroscopy' in chemico-physics, a domain to which an enormous volume of literature has been devoted (see for instance Barsoukov and MacDonald 2005). As far as geophysical applications are concerned, the explored frequency range lies between 10^{-3}Hz and 10^{4}Hz, although theses frontiers are fuzzy. At the lower end, the limiting factor results simply from the time needed for the measurements, especially because geophysicists need to acquire large quantities of data in order to derive an acceptable model of the subsurface. At the upper limit, the limiting factor is EM coupling, which is, in the language of geophysicists, the EM 'standard' response in the absence of a targeted, highly polarizable material of geophysical/geological/environmental interest. This is referred to as the 'coupling problem'. Some recent studies have proposed models involving coupling, in order to distinguish between various undesirable signals. As examples, Ingeman-Nielsen and Baumgartner (2006) provided tools for the modelling of these effects. Morgan and Lesmes (2004) discussed both inductive and capacitive coupling when applying IP to contaminant plumes, whereas Ghorbani *et al.* (2009) developed inversion techniques for the horizontally layered subsurface, which take coupling effects into account in the determination of the Cole-Cole parameters. The ERT inversion in 3D has also become a standard method and 3D IP has followed this progress. There are numerous noteworthy studies on the topic, including the pioneering research reported by Li and Oldenburg (2000) and the more recent work by Commer *et al.* (2011). Following the use of 2D IP tomography by Loke *et al.* (2006), Loke and Barker (1996) included 3D analysis in their well-known DC-IP code, devoted to ERT inversion, referred to as RES3DINV. This code was used in the analyses reported in the present paper.

Depending on the space and overall time available in the field, various electrode layouts can be used. An intuitive and efficient arrangement involves two perpendicular sets of parallel profiles, aligned along the x and y directions. Diagonal electrode locations may be added, to enrich the data set and further constrain the inverted resistivity and/or chargeability. It should be recalled that 3D information is already available in the form of a simple set of parallel panels ('x-3D' for instance), because the apparent resistivities involve lateral heterogeneity effects. The main point is: the inversion must be carried out using a 3D code, in order to include this lateral contribution in the raw data. A suitable discussion and example of x-3D, y-3D and xy-3D analysis can be found in Negri *et al.* (2008), which provide an example associating 3D imagery, IP and archaeology.

BRIEF DESCRIPTION OF THE SITE

The test area is named 'Castel-Minier' and is located in the Department of Ariège, France (42°46'20"N, 1°22'21"E). It was active from the end of the 12th century until *circa* 1580 and produced silver and iron. Two significant slag heaps were discovered by means of on-site prospection. They were studied using three different techniques: micro-topographic, pedological and magnetic. A detailed description can be found in Bonnamour *et al.* (2007), including the results of various geophysical investigations. In our previous paper (Florsch *et al.* 2011), we reported on the IP investigation carried out on the first slag heaps (2D only) and the 'ground-truth' checks derived from various excavations. Figure 1 shows the local context. In the present paper, we concentrate on the study of the second slag heaps, using our previous laboratory calibration, to derive a full 3D interpretation of the field measurements.

3D SCANNING OF THE SLAG HEAPS WITH IP AND VOLUME ESTIMATION

Instrumental strategy

In our aforementioned initial study, a Spectral Induced Polarization (SIP) profile was determined, in order to identify the spectral zone corresponding to the slags' response and in which we found that the characteristic time constant corresponds to approximately 1 Hz. We found that a Cole-Cole complex resistivity model provides a suitable fit to the spectral data. We preferred the use of 'traditional' time-domain IP, because it saves considerable time in the field and in practice is generally more robust. For the 3D survey reported here, the previously used

FIGURE 1
Photograph of the Castel-Minier site, showing the location of the buried slag heap under study.

acquisition procedure was maintained. We made use of the partial chargeability of an initial window [10 ms, 30 ms], thereby avoiding the need to fit the entire decay curve. We use this early window because it allows the parameter m of a Cole-Cole model (Cole and Cole 1941) to be computed directly from field data. Indeed, we recall that the Cole-Cole model corresponds to the frequency dependent resistivity of the form:

$$\rho(\omega) = \rho_0\left[1 - m\left(1 - \frac{1}{1+(i\omega\tau)^c}\right)\right] \quad (1)$$

where ρ_0 is the DC resistivity, τ is a characteristic time constant, c is a dispersion parameter (between 0–1) and m is the 'chargeability', which has the same physical dimensions as a concentration of polarizable material and also lies between 0–1. It should be noted that this form was initially proposed by Cole and Cole (1941) for the calculation of permittivity but has since been found to be suitable and useful for the modelling of complex resistivity responses to a wide range of geophysical applications. Recently, Florsch *et al*. (this issue, equation (35)) established a technique for switching between the resistivity and conductivity (or permittivity) Cole-Cole representations. In the following, we use the resistive formulation, because measurements in the time domain involve voltages that, as a result of Ohm's law, are dimensionally homogeneous with the resistivity.

Several authors, for example Kemna (2000), Luo and Zhang (1998), Routh *et al*. (1998) and Xiang *et al*. (2001), have proposed schemes to retrieve the Cole-Cole parameters from time- and frequency-domain measurements. At the present time, although it is still difficult to derive the Cole-Cole parameters from time-domain IP measurements (see Ghorbani *et al.* 2007, who revisited the inversion of the Cole-Cole parameters through Bayesian analysis), a simple method for retrieving m from the data, without the need to estimate all Cole-Cole parameters, can be derived from the partial chargeability (in ms), defined as:

$$M_{t_1,t_2} = \frac{1}{V_0}\int_{t_1}^{t_2} V(t)dt\,, \quad (2)$$

where V_0 is the potential just before the current cut-off and V(t) is the potential following current cut-off. Assuming $t_1 < t_2 << \tau$, it was shown in Florsch *et al.* (2011) that m (in %) can be estimated using:

$$m \cong \frac{M_{t_1,t_2}}{(t_2 - t_1)}\,. \quad (3)$$

From the time expression of the decay, related to the Cole-Cole model, it is known that the Cole-Cole parameter can also be evaluated as:

$$m = \frac{V_1}{V_0}\,, \quad (4)$$

where V_0 is the voltage just before cut-off and V_1 the voltage just after cut-off. This is also coherent and compatible with the definition given by Seigel (1959) and Seigel *et al.*(1997), who defined the chargeability m in terms of the residual voltage measured immediately after the shut-down of an impressed current, divided by the voltage observed just before shut-down of the current. The above procedure provides a simplified, robust and efficient estimation of m and avoids the difficulties associated with measuring the very early voltage decay after current shut-down, given a 10 ms delay before taking the signal into account. But a full approach should involve the alternative switching of positive and negative injected currents.

It should be noted that the partial chargeability given by equation (3) can also be considered as a simple empirical quantity, without any reference being made to a known analytical model (such as the Cole-Cole model), such that the main conclusions of the present paper are not affected by the use of one model or another.

In fact, it will not be necessary to compute m to characterize the slag heap but it should be noted that the partial chargeability M_{t_1,t_2} is directly and physically linked to m, since this will enforce the validity of converting M_{t_1,t_2} to a slag concentration, as shown by Florsch *et al.* (2011). In the latter paper, we report on a tank experiment in which a certain quantity of soil was taken from the ground in the field and to which an increasing and known quantity of slag, also taken from the field but separated by sorting from the surrounding earth, was added and mixed. Then, for each known slag concentration, the IP response was measured, whilst adjusting the same apparatus parameters as that used in the field (using the lowest voltage in order to avoid the occurrence of non-linearities). We were thus able to reproduce the field 'reality' by controlling both the quantity of slag and its partial chargeability. The experiment revealed a linear trend between the slag concentration C (in %) and the partial chargeability M_{t_1,t_2}, which is described by the following empirical relationship:

$$M_{t_1,t_2} = \alpha C + \beta\,. \quad (5)$$

In numerical terms, we found: α = 0.107 ms/kg/kg (or ms), β = 0.783 ms, with an R-squared coefficient of determination equal to 0.985.

Tomography results

3D tomography was performed in the time domain using an ABEM SAS1000 Terrameter. A simple Wenner electrode arrangement was chosen by using a set of parallel profiles, without involving perpendicular lines, i.e., the system sometimes referred to as 'y-3D'. The distance between the lines (1.5 m) is taken to be less than twice the electrode spacing (0.8 m) along a line and the data set of such an array involves the required 3D lateral information, assuming the structure not to be anisotropic.

We used non-polarizable Cu/CuSO4 electrodes with porous ceramics, as described in Florsch *et al.* (2011).

The layout with the set of parallel profiles is shown in Fig. 2, superimposed onto the magnetic map (Bonnamour 2007) and the surrounding topography. A magnetic sounding technique allowed the heaps to be initially discovered, due to the presence of magnetite embedded in the slag glass, resulting from chemical reduction processes of other iron oxides (Le Borgne 1960). An optically pumped gradiometer from Geometrics was used, with a spatial sampling interval of not more than one metre and with the combined use of 'walking' and 'point-by-point' modes, according to the local topography. Although the magnetic map proved to be very useful for the detection of slag heaps, it cannot be used to retrieve the depth of the body bottom and even less its volume.

We inverted the measured partial chargeabilities into images of intrinsic partial chargeabilities using RES3DINV software (Loke and Barker 1996) and converted the resultant image data into slag concentrations using the empirical relationship equation (5) above. In the inversion, topography was taken into account. The resulting data can then be directly converted to concentration values. The inverted data are shown in Fig. 3(a) (slices of resistivity), Fig. 3(b) (slices of chargeability), Fig. 4(a) (volume of resistivity) and Fig. 4(b) (volume of chargeability).

The compactness of the IP anomaly is striking, in particular when it is compared with the resistivity images. This is a feature of this method, when applied to slag heaps, which has already been observed by several authors.

Conversion to slag mass and volume and comparison with other estimations

To perform the estimation of the mass or volume of this slag heap, we took into account the volumes having chargeability greater than an arbitrary partial chargeability threshold T of 1.8 ms. Lower values were not considered because they occupy the surrounding large volume and would thus bias the integral obtained for the full studied volume. This rule of thumb was established in accordance with observations made in the field: no slag was found outside the boundary defined by this limit, as can be seen in the inverted image, which is also indicated by a colour contour in Fig. 3(b). We therefore consider that all points lying outside this limit are external to the heap. Although the choice of a somewhat arbitrary threshold will have a small effect on the final mass estimation (underestimation), excessive integration of the background noise can also lead to an overestimation of the slag mass. The question of selecting the optimal threshold limit is of course case-dependant and should be decided according to the specific context of each archaeological site. The chargeability is obtained as a function of the space coordinate (x,y,z), as an output of RES3DINV. It can be directly converted into volume concentration using the calibration factor obtained in Florsch *et al.* (2011), which was obtained from the first heap investigated on the site. The latter paper also provides the calibration procedure, as described above in Instrumental strategy .

Numerically speaking, with M_{t_1,t_2} expressed in ms and the concentration C in % (more precisely as 100 X [kg of slag]/[total

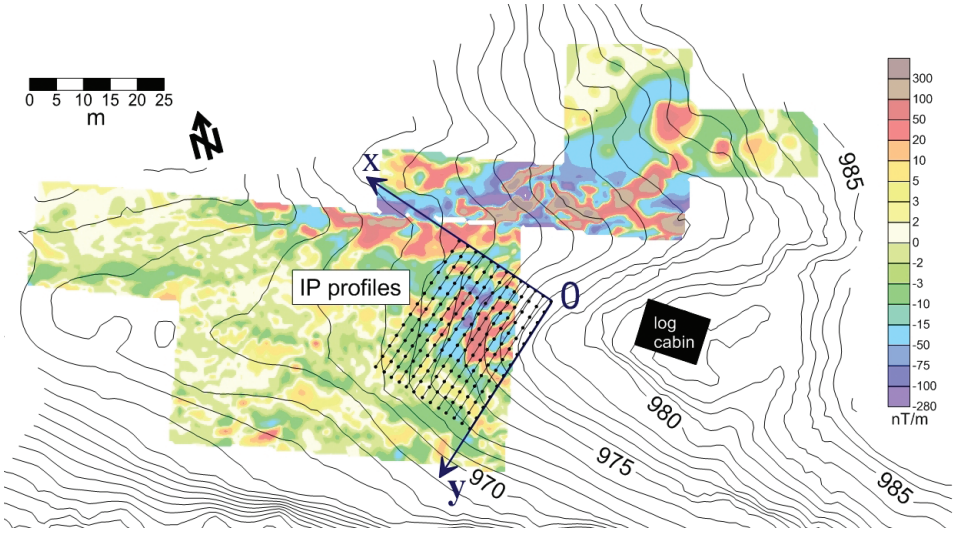

FIGURE 2
Location and orientation of the thirteen 'y parallel-3D' profiles used for 3D tomography, superimposed onto the magnetic map (vertical gradient nT/m, see Bonnamour *et al.* 2007) and the surrounding topography.

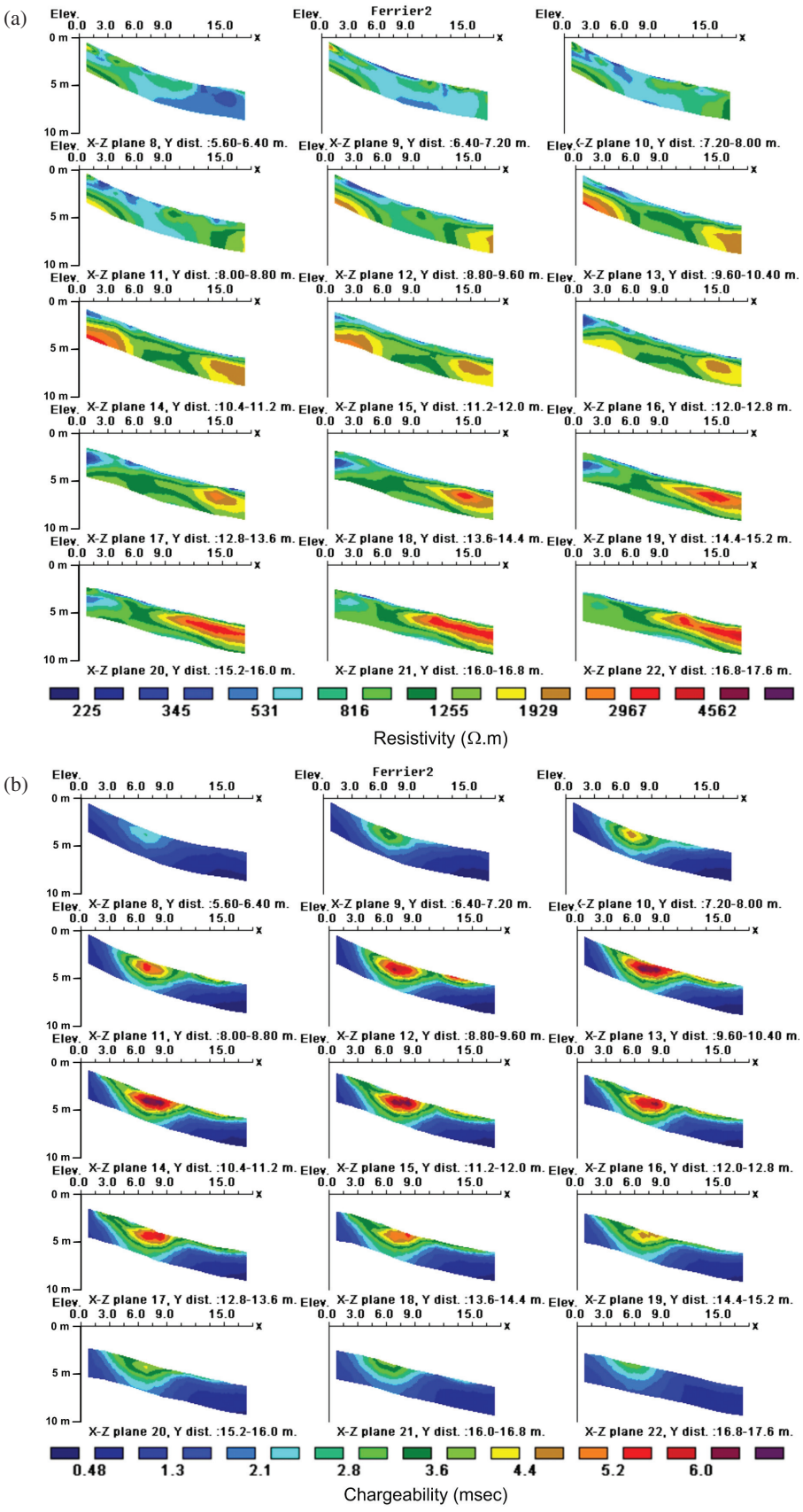

FIGURE 3
a) 3D tomography of the slag heap by slices: resistivity, b) 3D tomography of the slag heap by slices: chargeability

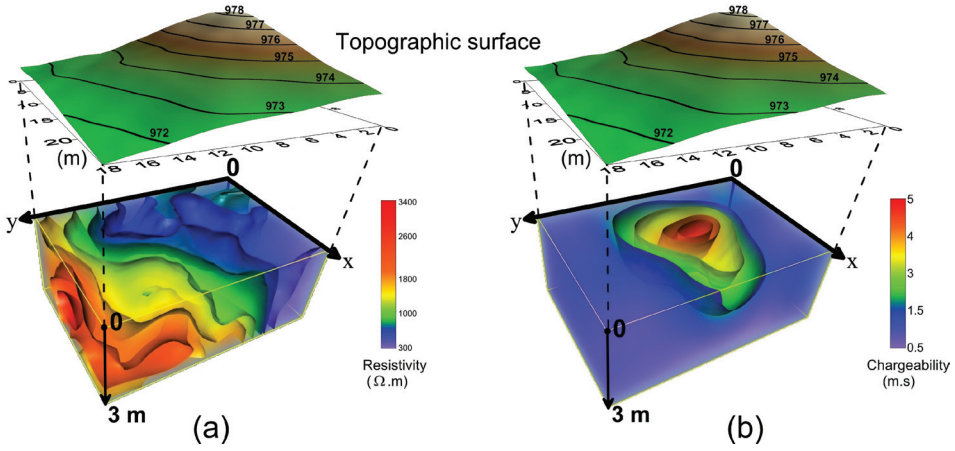

FIGURE 4
3D tomography of the slag heap in volume: (a) resistivity and (b) chargeability. The height of the topography with respect to the 3D structure is not to scale.

weight in kg]), we have:

$$C(x,y,z) = \frac{\left[M_{t_1,t_2}(x,y,z) - 0.78\right]}{10.73}. \quad (6)$$

Notice that since the densities of slags and soil are not distinguishable, the concentration in terms of volume is the same by chance. Finally, the total slag volume is obtained by numerical integration, involving the volume of each cell (v_i) as calculated by RES3DINV and the chargeability (C_i) in this cell. The same approach can be used to determine the mass of the slag. Mathematically, these two quantities can be written as:

$$M_{slags} = \iiint_{I(M\geq 1.8)} \rho_{slag} C(x,y,z)\,dxdydz \cong \rho_{slag} \sum_i I_i C_i v_i , \quad (7)$$

or similarly:

$$V_{slags} = \iiint_{I(M\geq 1.8)} C(x,y,z)\,dxdydz \cong \sum_i I_i C_i v_i , \quad (8)$$

where $I_i = 1$ if $M_{t_1,t_2} \geq T = 1.8$ ms and 0 elsewhere. The studied area involves 2232 cells, of which only 500 have a concentration above the defined threshold. In this restricted volume, the mean slag concentration is 21%. As the specific weight of the soil and the slag material are both very close to 2000 kg/m^3, we obtain a mass of 127 tons of slag, for a volume V = 63.5m^3.

An initial, independent estimation of the volume of this heap was previously obtained by Bonnamour *et al.* (2007). The minimal volume was estimated to be approximately V = 60m^3; however several biases may have affected this estimation: firstly, the volume could have been overestimated, since it was based on the assumption of a concentrated slag mix, rather than on pure slag. Secondly, it is also possible that it was underestimated, because a hand auger only 1.5 m in length was used, which was unable to reach the very bottom of the heap.

Furthermore, an excavation of 6 x 1 x 1.5 m^3 was made in 2005, which did not fully delimit the heap but allowed it to be confirmed that the base of the slag heap has a depth of more than 1.6 m. By extrapolating the shape of the heap's lower boundary, we can assume that its base is 40 cm lower than the initially estimated value of 1.6 m. This is in agreement with what can be derived from the IP survey.

Finally, the mass of iron produced at a given slag heap can also be estimated, using the same procedure as that described in Florsch *et al.* (2011). This leads to a value lying in the range between 36–50 tons of iron (for the heap described in this study only).

Error estimation

Several sources of uncertainty merit discussion:

- Some errors can arise from the intrinsic variability of the IP response, with respect to a given slag mass. Such errors can in some cases lead to strong uncertainties, due to the use of a calibration coefficient, which is estimated from a particular sample taken in the field.
- Some uncertainties can arise from the integral calculation. We consider the product given by: (VOLUME) X (CONCENTRATION) to be less variable in terms of percentages than the multipliers. Although subsurface imaging smoothes the reality, it preserves more or less the integral. This might be not general but was found for heap number one and we suppose it is still valid in the present case. However, we performed a synthetic test made with an equivalent but flat volume (5 x 5 x 1.5 m^3), a body with chargeability 5 ms, embedded in a background with chargeability 1 ms and assuming the same threshold of 1.8 ms. The 'true' integral equalled 187.5 m^3 while the estimated integral from the data inverted from the IP modelling was 231 m^3, which is 19% in excess. A specific study can be done in the future to better understand why we actually obtained better results on the field than with synthetic modelling.
- Some errors can arise due to equivalence effects or to a loss in sensitivity in the deeper portions of the slag heap. The main requirement is to ensure that the current flow not only traverses but also surrounds the targeted structure. This can be affected by the choice of electrode array, by the surveyed area and also by the resistivity contrast in cases where the current is channelled.

Although we are aware of the more advanced approaches to assess electrical image uncertainty, in particular involving sensitivity and resolution (see e.g., Day-Lewis *et al.* 2005; Nguyen et al. 2009),

we here followed a pragmatic approach and compared the imaging results with the results of the excavation of a nearby slag heap (Florsch *et al*. 2011). This provides a considerable degree of 'ground truth' (which does not however alleviate the difficulties generally encountered during such campaigns). The quantity of slag determined by the archaeological dig was in surprisingly good agreement with the quantity estimated with the IP imaging method. This comparison leads us to assume a 20% uncertainty as the upper limit of the estimated slag mass in the present study.

DISCUSSION AND CONCLUSION

The aim of this paper is to provide a 3D validation of a tomographic procedure used with slag heaps from ancient mine settlements. Clearly, the IP method is very efficient and probably one of the best currently available geophysical imaging techniques for such a task. Not only a reliable geometrical delimitation can be obtained but moreover the method makes it possible to estimate the entire mass of buried slag heap material. The question as to what minerals or aggregates are responsible for this IP signal still remains to be answered. Because of the overlapping of the IP anomaly with the magnetic anomaly and because the slags involved here are iron residues and magnetite is known to show an IP response, we suspect this mineral to be the source of electrode polarization effects, when dealing with such a slag heap target. This has been confirmed by a very recent study not shown here, in which we separated the magnetite particles from the slag and confirmed their strong IP response. However, the mineral phases present in slags may be complex and this question relating to the source of the IP signal, which provides such good results in terms of tomography, thus calls for further investigation.

ACKNOWLEDGEMENTS

This final redaction of the project benefited from Andreas Kemna's benevolence and encouragements and of the constructive suggestions and corrections provided by the three reviewers Andreas Weller, Konstantin Titov and Gianluca Finadaca. The field work was funded by the French Ministry of Culture thanks to DRAC-SRA Midi-Pyrénées (France).

REFERENCES

Aspinal A. and Lunam J. 1968a. Induced polarization as a technique for archaeological surveying. *Prospezioni Archeologiche* **3**, 91–93.

Aspinal A. and Lunam J. 1968b. An induced polarization instrument for the detection of near-surface features. *Prospezioni Archeologiche* **5**, 67–75.

Barsoukov E. and Macdonald J.R. 2005. *Impedance Spectroscopy: Theory, Experiment, and Applications*. Wiley-Interscience, 2nd edition, p. 616. ISBN-10: 0471647497 and ISBN-13: 9780471647492.

Bonnamour G., Florsch N. and Téreygeol F. 2007. Les prospections des ferriers de Castel-Minier: Approche interdisciplinaire. *ARCHEOSCIENCES, revue d'Archéométrie* **31**, 37–44.

Cole K.S. and Cole R.H. 1941. Dispersion and absorption in dielectrics, I. Alternating current fields. *Journal of Chemical Physics* **9**, 341–353.

Commer M., Newman G.A., William K.H. and Hubbard S.S. 2011. 3D induced-polarization data inversion for complex resistivity. *Geophysics* **76**, 157–171. doi: 10.1190/1.3560156

Day-Lewis F.F., Singha K. and Binley A.D. 2005. Applying petrophysical models to radar travel time and electrical resistivity tomograms: Resolution-dependent limitations. *Journal of Geophysical Research* **110**, B08206. doi:10.1029/2004JB003569.

Decombeix P.-M., Fabre J.-M., Tollon F. and Domergue Cl. 1998. Evaluation du volume des ferries romains du domaine des Forges (Les Martys, Aude), de la masse de scories qu'ils renferment et de la production de fer correspondante. *ARCHEOSCIENCES, revue d'Archéomètrie* **22**, 77–90.

Domergue C. and Leroy M. 2000. Mines et métallurgie en Gaule, recherches récentes. *Gallia* **57**, 158.

Florsch N., Camerlynck C. and Revil A. 2012. Direct estimation of the distribution of relaxation times from induced-polarization spectra using a Fourier transform analysis. *Near Surface Geophysics* **10**(6). doi:10.3997/1873-0604.2012004.

Florsch N., Llubes M., Téreygeol F., Ghorbani A. and Roblet P. 2008. Quantification of buried slag volumes by using non-invasive geophysical methods. *Proceedings of the 1st International EARSeL Workshop, CNR*, Rome, September 30–October 4, 2008.

Florsch N., Llubes M., Téreygeol F., Ghorbani A. and Roblet P. 2011. Quantification of slag heap volumes and masses through the use of induced polarization: application to the Castel-Minier site. *Journal of Archaeological Science* **38** (2), 438–451. doi:10.1016/j.jas.2010.09.027.

Ghorbani A., Camerlynck C. and Florsch N. 2009. CR1Dinv: A Matlab program to invert 1D spectral induced polarization data for the Cole-Cole model including electromagnetic effects. *Computers & Geosciences* **35**, 255–266.

Ghorbani A., Camerlynck C., Florsch N., Cosenza P. and Revil A. 2007. Bayesian inference of the Cole-Cole parameters from time- and frequency-domain induced polarization. *Geophysical Prospecting* **55**, 589–605. doi:10.1111/j.1365-2478.2007.00627.x

Ingeman-Nielsen T. and Baumgartner F. 2006. CR1Dmod: A Matlab program to model 1D complex resistivity effects in electrical and EM surveys. *Computers & Geosciences* **32**, 1411–1419.

Kemna A. 2000. Tomographic inversion of complex resistivity: Theory and application. Onsnabrück: Der Andere verlag 2000. Berichte des Institutes für Geophysik der Ruhr-Universität Bochum: Reihe 1; Nr. 56. Zugl. : Bochum, Der Andere Verlag; Reihe 1; Ruhr-Universität, Diss., 2000. ISBN 3-934366-92-9.

Kemna A. and Binley A. 1996. Complex electrical resistivity tomography for contaminant plume delineation. *Proceedings of 3rd Annual Meeting, Environmental and Engineering Geophysics, EEGS*, Expanded Abstracts, 151–154.

Kemna A., Binley A. and Slater L. 2004. Crosshole IP imaging for engineering and environmental applications. *Geophysics* **69**, 97–107.

Le Borgne E.1960. Influence du feu sur les propriétés magnétiques du sol et sur celles du schiste et du granite. *Annales de Geophysique* **16**, 159–195.

Li Y. and Oldenburg D.W. 2000. 3-D inversion of induced polarization data. *Geophysics* **65**, 1931–1945. [ISI] doi:10.1190/1.1444877

Loke M.H. and Barker R.D. 1996. Practical techniques for 3D resistivity surveys and data inversion. *Geophysical Prospecting* **44**, 499–523.

Loke M.H., Chambers J.E. and Ogilvy R.D. 2006. Inversion of 2D spectral induced polarization imaging data. *Geophysical Prospecting* **54**, 287–301.

Luo Y. and Zhang G. 1998. *Theory and Application of Spectral Induced Polarization*. Geophysical Monograph Series. Edited by Society of Exploration Geophysicists.

Morgan F.D. and Lesmes D. 2004. Induced Polarization with Electromagnetic coupling: 3D Spectral Imaging Theory. EMSP Project No. 73836, U.S. Department of Energy, Environmental Management Science Program, Washington, D.C. Available online at http://emsp.em.doe.gov/

Negri S., Leucci G. and Mazzone F. 2008. High resolution 3D ERT to help GPR data interpretation for researching archaeological items in a geologically complex subsurface. *Journal of Applied Geophysics* **65**, 111–120. doi:10.1016/j.jappgeo.2008.06.004.

Nguyen F., Kemna A., Antonsson A., Engesgaard P., Kuras O., Ogilvy R. *et al*. 2009. Characterization of seawater intrusion using 2D electrical imaging. *Near Surface Geophysics* **7**, 377–390.

Routh P.S., Oldenburg D.W. and Li Y. 1998. Regularized in version of spectral IP parameters from complex resistivity data. *SEG Expanded Abstracts* **17**, 810. http://dx.doi.org/10.1190/1.1820608

Schleifer N., Weller A., Schneider S. and Junge A. 2002. Investigation of a Bronze Age plankway by spectral induced polarisation. *Archaeological Prospection* **9**, 243–253.

Seigel H.O. 1959. Mathematical formulation and type curves for induced polarization. *Geophysics* **24**, 547–565.

Seigel H.O., Vanhala H. and Sheard S.N. 1997. Some case histories of source discrimination using time-domain spectral IP. *Geophysics* **62**, 1394–1408.

Ullrich B., Meyer C. and Weller A. 2007a. Geoelektrik und Georadar in der Archäologischen Forschung: Geophysikalische 3D-Untersuchungen in Munigua (Spanien). In: *Einführung in die Archäometrie* (ed. G.A. Wagner), pp. 76–93. Springer-Verlag Berlin, Heidelberg.

Ullrich B., Weller A., Günther T. and Rücker C. 2007b. Geophysical prospecting of ancient slag deposits in Munigua (Spain) and Ain-al Hajer (Morocco) using complex resistivity tomography. 2nd International Conference Archaeometallurgy in Europe – Aquileia (Italy) 2007.

Weller A. 2003. Spektrale induzierte Polarisation in der Archäometrie. Freiberger Forsch.-Hefte C496, 14–29.

Weller A., Brune S., Hennig T. and Kansy A. 2000. Spectral induced polarisation at a medieval smelting site. 6th Meeting of the Environmental and Engineering Geophysical Society (European Section), Bochum 2000.

Xiang J., Jones N.B., Cheng D. and Schlindwein F.S. 2001. Direct inversion of the apparent complex-resistivity spectrum. *Geophysics* **66**, 1399–1404.